Research article

Journal of RAMAN SPECTROSCOPY

Received: 25 January 2012 Revised: 11 April 2012 Accepted: 5 June 2012 Published online in Wiley Online Library: 2 August 2012

(wileyonlinelibrary.com) DOI 10.1002/jrs.4141

Observation of low-wavenumber out-of-plane optical phonon in few-layer graphene

Jingzhi Shang,[a] Chunxiao Cong,[a] Jun Zhang,[a] Qihua Xiong,[a,b] Gagik G. Gurzadyan[a]* and Ting Yu[a,c,d]*

Few-layer graphene grown by chemical vapor deposition has been studied by Raman and ultrafast laser spectroscopy. A low-wavenumber Raman peak of ~120 cm^{-1} and a phonon-induced oscillation in the kinetic curve of electron–phonon relaxation process have been observed, respectively. The Raman peak is assigned to the low-wavenumber out-of-plane optical mode in the few-layer graphene. The phonon band shows an asymmetric shape, a consequence of so-called Breit-Wigner-Fano resonance, resulting from the coupling between the low-wavenumber phonon and electron transitions. The obtained oscillation wavenumber from the kinetic curve is consistent with the detected low-wavenumber phonon by Raman scattering. The origin of this oscillation is attributed to the generation of coherent phonons and their interactions with photoinduced electrons. Copyright © 2012 John Wiley & Sons, Ltd.

Supporting information may be found in the online version of this article.

Keywords: few-layer graphene; Raman scattering; ultrafast spectroscopy; coherent phonon

Electronic and vibrational properties of bulk graphite have been investigated for more than 50 years. In the past few years, graphene, i.e. two-dimensional carbon, has attracted extensive efforts in both fields of fundamental physics and applications.[1] Recently, few-layer graphene, a transitional material structure, has started to become a hot topic as a candidate for discovering the evolution of structures and properties from graphene to graphite.[2,3] Previously, Raman spectroscopy plays an important role in determination and characterization of the phonon modes in graphene and graphite,[4–8] where considerable Raman scattering features have been clarified.[4,5] Studies of various phonon modes are critical to understand the basic electron–phonon scattering processes in graphene films such as hot phonon decay.[9] According to the group theory, graphene and graphite have six and twelve normal phonon modes at the Brillouin zone center (Γ point), $A_{2u} + B_{2g} + E_{1u} + E_{2g}$ and $2A_{2u} + 2B_{2g} + 2E_{1u} + 2E_{2g}$, respectively.[4] Therein, only one E_{2g} mode (~1580 cm^{-1}) is Raman active in graphene while two E_{2g} modes (~1580 and 42 cm^{-1}) are Raman active in graphite.[10] Recently, theoretical studies predict that the Raman inactive low-wavenumber B_{2g} mode in graphite and graphene could become Raman-active optical phonon modes in the few-layer graphene films, and those modes are sensitive to the number of layers.[10–12] Jiang *et al*. predicted that a low-wavenumber interlayer optical mode is Raman or infrared active in even or odd multilayer graphene films, respectively.[12] Saha *et al*. anticipated a ~112 cm^{-1} optical phonon mode in ultrathin graphene films by the first-principles study.[10] Malard *et al*. found that some small wavenumber out-of-plane modes were Raman active by the group-theory analysis.[11]

Experimentally, the low-wavenumber Raman spectroscopy was not used to investigate the Dirac point physics in graphene because of the absence of Raman-active phonon modes in this range. Nevertheless, it could become a promising tool to provide wealth information on electrons, phonons and their interactions around the intrinsic Fermi level in few-layer graphene. A recent report has successfully uncovered a low-wavenumber shear mode (31 to 43 cm^{-1}) by Raman spectroscopy in the multilayer graphene.[13] On the other side, the ultrafast laser pump-probe spectroscopy has also presented a unique ability to generate and detect the low-wavenumber vibration mode in carbon materials.[14] These works inspirit us to determine the interlayer modes by low-wavenumber Raman scattering and ultrafast laser pump-probe technique.

It is noted that early neutron scattering measurements confirmed the existence of the low-wavenumber B_{2g} mode in graphite;[15] however, the direct experimental observation of the corresponding vibration mode in few-layer graphene films has not been reported in detail. In this work, we focus on the low-wavenumber out-of-plane optical phonon in few-layer graphene films grown by chemical vapor deposition (CVD). This

* *Correspondence to: Gagik G. Gurzadyan, Division of Physics and Applied Physics, School of Physical and Mathematical Sciences, Nanyang Technological University, Singapore 637371. E-mail: gurzadyan@ntu.edu.sg*
Ting Yu, Graphene Research Centre, National University of Singapore, 2 Science Drive 3, Singapore 117542. E-mail: yuting@ntu.edu.sg

a *Division of Physcs and Applied Physics, School of Physical and Mathematical Sciences, Nanyang Technological University, Singapore, 637371*

b *Division of Microelectronics, School of Electrical and Electronic Engineering, Nanyang Technological University, Singapore, 639798*

c *Department of Physics, Faculty of Science, National University of Singapore, Singapore, 117542*

d *Graphene Research Centre, National University of Singapore, 2 Science Drive 3, Singapore, 117542*

Journal of RAMAN SPECTROSCOPY

mode is clearly observed by both low-wavenumber Raman and ultrafast laser pump-probe spectroscopy. The Raman peak exhibits an asymmetric feature which is due to the coupling between the electronic transitions and Raman scattering. The oscillation of the electron–phonon relaxation process is related to the generation of coherent phonons. By Fourier transformation, the obtained wavenumber from the kinetic curve agrees well with the Raman peak of low-wavenumber out-of-plane phonon in the few-layer graphene.

Experimental

Few-layer graphene was grown on the copper foil by using low-pressure thermal CVD. The growth mechanism is a surface-catalyzed process, and the low solubility of carbon in copper is important for controlling the thickness of graphene film.[16,17] At first, the high temperature annealing at 1000 °C for 15 min was carried out under H_2 (10 sccm) and Ar (20 sccm) mixed atmosphere to remove surface oxide layers. Later on, instead of supplying Ar gas above, 50-sccm methane was used as the carbon source. After 2 h, few-layer graphene on copper foil was formed under a growth pressure of 4.6 Torr. The obtained few-layer graphene together with the copper substrate was put in the aqueous solution of iron nitride $(FeNO_3)_3$ for etching the copper foil. At last, the floating few-layer graphene was transferred onto a silicon substrate with see-through holes. The suspended few-layer graphene over the hole was used in the following measurements. Number of layers in the CVD-grown graphene sample has been characterized by three independent methods: atomic force microscopy, Raman and UV-visible absorption spectroscopic techniques. The used CVD grown graphene film consists of three to four layers. The details have been provided in Supporting Information (Fig. S1, S2 and S3). More information of the similar suspended graphene samples can be found in our recent work.[18]

A WITec Raman system (CRM 200) with a diode-pumped frequency-doubled Nd:YAG laser (532 nm) was employed to measure Raman spectra in the high-wavenumber regions. The weak Raman signals between 1650 and 1850 cm^{-1} were measured by a 532-nm Renishaw Raman system with a 2400 lines/mm grating. A Horiba-JY Raman system (T 64000) was used to detect the low-wavenumber Raman signals at an excitation wavelength of 632.8 nm. For ultrafast pump-probe measurements, the 800-nm output of titanium–sapphire (Legend Elite, Coherent) regenerative amplifier seeded by an oscillator (Micra, Coherent) was used as a pulse laser source: pulse width 80 fs, pulse repetition rate 1 kHz and average power 2.6 W. The 90% of the radiation was converted into 680-nm excitation pulses by passing an optical parametric oscillator which was used as the pump beam. The rest 10% was used to obtain the probe radiation in the range of 350–850 nm through with-light-continuum generation in CaF_2 plate; it was further divided into two beams for producing sample and reference signals, respectively. A mechanical delay stage of optical path was used to vary the time interval between the pump and the probe pulses. By focusing pump and probe pulses on the same region of sample, the transient transmission changes were induced. Two spectrographs with attached diode arrays (Model 77400, Oriel) were arranged to detect sample and reference signals. Thus, transient transmission data were obtained both as spectra and kinetics. Here, the pronounce signal was detected with the excitation beam of 680 nm and the probe wavelength of 778 nm. The full width at half maximum (FWHM) of the instrument response function was 90 ±10 fs. The details of the pump-probe system are described in previous studies.[19,20]

Results and discussion

Figure 1 shows the Raman spectra of the CVD-grown graphene films in the high-wavenumber range. G and G′ (also called 2D) bands were observed in 1L, 2L and few-layer graphene films grown by CVD as shown in Fig. 1a, which came from two in-plane optical phonons related to the first-order Raman scattering and the two-phonon double resonance process, respectively.[5] With the increase in the number of layers, the G′ band shifts to the high wavenumber and becomes broader. Meanwhile, the integrated peak intensity ratio of G to G′ increases. Particularly, in the range from 1650 to 1850 cm^{-1}, the weak M band was detected in the CVD-grown few-layer graphene, and the Raman spectra of the mechanically exfoliated AB stacked 1-3L graphene samples were also presented for comparison as shown in Fig. 1b. The recent studies assign the M band to the second-order overtone out-of-plane transverse mode which is absent in monolayer graphene and non-AB stacked bilayer graphene.[21,22] The presence of M band approves that there are AB-stacked layers in the CVD-grown graphene films. Moreover, the data from 19 random regions on the CVD-grown few-layer graphene films have been shown in Fig. 1c and 1d, where the FWHM of G′, the

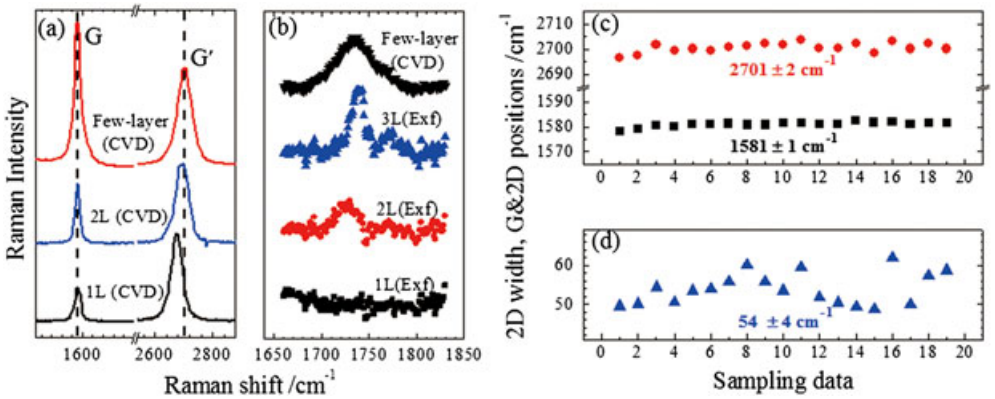

Figure 1. (a) Raman G and G′ (2D) bands of CVD-grown 1L, 2L and few-layer graphene films. (b) Raman M bands of 1-3L mechanically exfoliated graphene films and the CVD-grown few-layer graphene. (c,d) The statistic data of G and G′ bands for the CVD-grown few-layer graphene.

positions of G and G′ bands are 54 ± 4, 1581 ± 1 and 2701 ± 2 cm^{-1}, respectively. Those features of Raman bands are consistent with the characteristics of the few-layer graphene grown by CVD in previous studies.[16,17]

Figure 2 presents the low-wavenumber Raman spectrum collected from the CVD-grown few-layer graphene film. Remarkably, an asymmetric Raman peak was found to be around 120 cm^{-1}. The origin of this peak in the few-layer graphene is assigned to the low-wavenumber out-of-plane optical phonon at Γ point in the Brillouin zone, as shown in Fig. 2b. Previously, it is known that the Raman activity of this phonon mode is silent in graphite, and it is nonexistent in graphene.[4] Nevertheless, for the few-layer graphene, this out-of-plane vibration mode can be Raman-active according to the calculations[10–12] based on the group theory. The asymmetric feature of this phonon peak indicates the Breit-Wigner-Fano (BWF) resonance between the phonon and electron transitions around the touching region of conduction and valence bands.[23] This Fano-type interference has also been observed for the tangential G band of the metallic carbon nanotube[24] and the low-wavenumber shear modes of multilayer graphene.[13] The obtained peak was fitted by a BWF function[23] with a linear baseline as below:

$$I(\omega) = I_0 + I_1\omega + I_2\frac{\left[1+\lambda^2+2(\omega-\omega_{\max})\lambda/\Gamma\right]^2}{\left[1+4(\omega-\omega_{max}+\lambda\Gamma/2)^2/\Gamma^2\right]} \quad (1)$$

where ω_{max}, Γ and λ are the BWF peak position at the maximum intensity, the pristine FWHM of the phonon band without the BWF resonance and the Fano-type interference constant, respectively.[13,23,24] In our case, ω_{max}, Γ and λ are 120 ± 1 cm^{-1}, 10 ± 3 cm^{-1} and −0.4 ± 0.03, respectively. Furthermore, ω_{max} is equal to $\omega_0 + \lambda\Gamma/2$[13], where ω_0 (~122 cm^{-1}) is the pristine peak position of this phonon when the intensity is $I_0 + I_1\omega_0 + I_2$. The positive or the negative sign of λ indicates the maximum intensity is located in the higher or the lower wavenumber in respect to ω_0. After the baseline correction, the FWHM of this peak is equal to $\Gamma(1+\lambda^2)/|1-\lambda^2|$, where the factor $(1+\lambda^2)/|1-\lambda^2| = 1.4$ can be used to evaluate the broadening of the phonon band. In other words, the observed FWHM is 1.4 times of the pristine FWHM of this mode. The low-wavenumber Raman spectrum of the suspended few-layer graphene samples prepared from graphite flakes by one-step heating[25] also shows the similar asymmetric Raman peak (see supporting information: Fig. S4), which further confirms the existence of the Raman-active out-of-plane phonon in the few-layer graphene.

Figure 3 shows the kinetic curve of transmission change (normalized to the initial transmission) of the CVD-grown few-layer graphene recorded by ultrafast laser pump-probe spectroscopy. The signal presents an optical bleaching feature, and it decays in the subsequent 2 ps, which is consistent with the previous reports.[19,26] In detail, the positive ΔT/T indicates the induced transmission by the pump pulse, and the intensity of ΔT/T reflects the information of carrier population in the probed electronic state. Decay of ΔT/T with the pump-probe delay time represents the carrier relaxation mainly due to carrier-optical

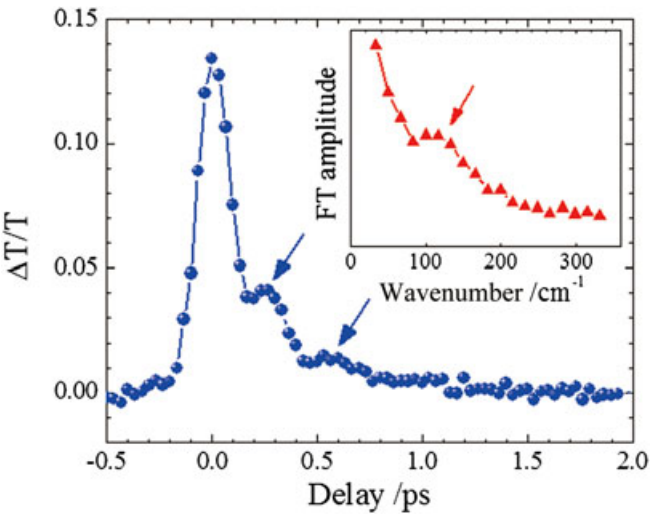

Figure 3. The kinetic curve of transmission change of the CVD-grown few-layer graphene with pump and probe wavelengths at 680 and 778 nm, respectively. The inset is Fourier transform amplitude *versus* wavenumber.

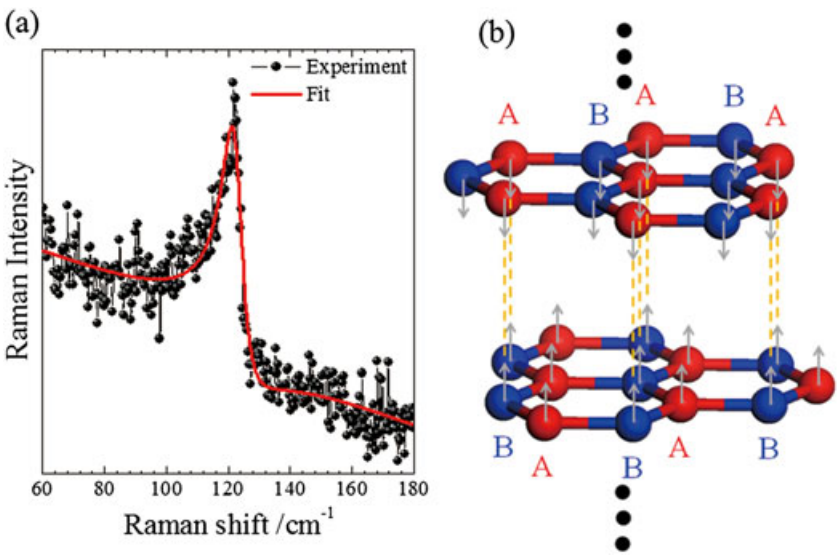

Figure 2. (a) The low-wavenumber Raman spectrum from the CVD-grown few-layer graphene and (b) the schematic pattern of atomic displacements for the low-wavenumber out-of-plane optical phonon.

phonon and optical phonon-acoustic phonon scattering. Strikingly, the amplitude of ΔT/T behaves an unambiguous oscillation with the delay time. The estimated time interval is 270 ± 30 fs, which corresponds to a wavenumber of 124 ± 15 cm^{-1}. The corresponding Fourier transform amplitude *versus* wavenumber further confirms this result as shown in the inset, where a peak around 120 cm^{-1} is indicated by the red arrow. This wavenumber is essentially coincident with the observed low-wavenumber out-of-plane optical phonon in the Raman spectrum above. The modulation of decay dynamics originates from the coherent coupling between excited electrons and lattice vibrations. Those coherent out-of-plane optical phonons were produced only during the laser excitation by pump pulses, different from the incoherent phonons created during hot electron cooling processes.[27] Moreover, the maximum amplitude of ΔT/T turns up at the delay time of 0 ps and the oscillation of ΔT/T follows a cosine function relationship of time. Note that the current finding is complementary to the recent observation[28] of high-wavenumber coherent phonons (1580 and 1350 cm^{-1}) in epitaxial graphene layers induced by ultrafast laser excitation. The high-wavenumber coherent phonons (1580 and 1350 cm^{-1}) were not observed here because the oscillation periods (21 fs and 25 fs) are smaller than the instrument-limited minimum scan step (~30 fs) of the delay time.

By use of ultrafast laser pulses, the coherent phonons were observed in a number of materials such as Bi, Sb, GaAs, graphite.[29–31] The possible generation mechanisms of coherent phonons have been proposed and discussed in the literatures.[29,32–38] Among these studies, two theories received extensive attention: impulsive stimulated Raman scattering (ISRS)[32] and displacive excitation of coherent phonons (DECP).[29] For the transparent materials to laser pulses, the former ISRS can be used to explain the origin of coherent phonons.[34] The latter DECP was developed for the opaque materials to laser pulses which showed the oscillations only caused by coherent A_1 (fully symmetric) modes.[29] In other words, DECP required the materials had real absorption in the excitation regions. Moreover, the significant controversy between ISRS and DECP is about the essence of excitation mechanisms: impulsive or displacive. The corresponding driving forces of excitations can be represented by the δ function- or the step function-like expression, respectively.[27] Later on, due to the findings of oscillation behaviors caused by coherent E_g, E_{2g} and T_{2g} in opaque materials,[31,35,38] the extended models based on both mechanisms have been developed.[34,35,37] In our case, first of all, the few-layer graphene films are opaque to the excitation wavelength. Moreover, according to the theoretical analysis in Ref. 10 and 11, it is found that the Raman-active low-wavenumber out-of-plane modes are A_{1g} and A'_1 modes for the few-layer graphene films with even and odd layers, respectively, and both modes are fully symmetric. Another feather is that the oscillation of ΔT/T intensity with time obeys the cosine function dependence. Thus, the observed oscillation in kinetic curve can be interpreted in terms of DECP.[29] Identically, in the single-walled carbon nanotubes, the DECP model was also suggested to explain the modulated kinetic curve caused by the low-wavenumber radial breathing phonons.[14]

Conclusion

To sum up, the low-wavenumber out-of-plane optical phonon has been studied in the CVD-grown few-layer graphene by Raman and ultrafast laser spectroscopy. The asymmetric (BWF lineshape) Raman peak of this mode was ascribed to the coupling between the phonon and electronic transitions, where the pristine phonon wavenumber, the Fano-type interference constant and the band broaden parameter are estimated to be ~122 cm^{-1}, −0.4 and 1.4, respectively. Ultrafast pump-probe measurements present a periodically modulated kinetic curve, which is due to the generation of coherent optical phonons and their coupling to the excited electrons. The obtained time interval is 270 ± 30 fs which corresponds to a wavenumber of 124 cm^{-1}, consistent with the Raman results. At last, the generation mechanism of coherent phonons in few-layer graphene was discussed by comparing existed theoretical models.

Acknowledgments

We thank Professor Maria-Elisabeth Michel-Beyerle for continuous support and Professor Jianyi Lin for providing the CVD system. Shang thanks Dr. Zhiqiang Luo and Dr. Haomin Wang for their fruitful discussions. Yu thanks the support of the Singapore National Research Foundation under NRF Award No. NRF-RF2010-07 and MOE Tier 2 MOE2009-T2-1-037. Q.X. acknowledges the support from Singapore National Research Foundation under NRF fellowship award (NRF-RF2009-06) and start-up grant from Nanyang Technological University (M58113004).

Supporting Information

Supporting information may be found in the online version of this article.

References

[1] A. K. Geim, K. S. Novoselov, *Nat. Mater.* **2007**, *6*, 183.
[2] M. F. Craciun, S. Russo, M. Yamamoto, J. B. Oostinga, A. F. Morpurgo, S. Tarucha, *Nat. Nanotechnol.* **2009**, *4*, 383.
[3] F. Zhang, J. Jung, G. A. Fiete, Q. Niu, A. H. MacDonald, *Phys. Rev. Lett.* **2011**, *106*, 156801.
[4] S. Reich, C. Thomsen, *Phil. Trans. R. Soc. Lond. A* **2004**, *362*, 2271.
[5] L. M. Malard, M. A. Pimenta, G. Dresselhaus, M. S. Dresselhaus, *Phys. Rep.* **2009**, *473*, 51.
[6] Y. You, Z. Ni, T. Yu, Z. X. Shen, *Appl. Phys. Lett.* **2008**, *93*, 163112.
[7] Z. H. Ni, T. Yu, Y. H. Lu, Y. Y. Wang, Y. P. Feng, Z. X. Shen, *ACS Nano* **2008**, *2*, 2301.
[8] C. X. Cong, T. Yu, H. M. Wang, *ACS Nano* **2010**, *4*, 3175.
[9] P. J. Hale, S. M. Hornett, J. Moger, D. W. Horsell, E. Hendry, *Phys. Rev. B* **2011**, *83*, 121404(R).
[10] S. K. Saha, U. V. Waghmare, H. R. Krishnamurthy, A. K. Sood, *Phys. Rev. B* **2008**, *78*, 165421.
[11] L. M. Malard, M. H. D. Guimarães, D. L. Mafra, M. S. C. Mazzoni, A. Jorio, *Phys. Rev. B* **2009**, *79*, 125426.
[12] J.-W. Jiang, H. Tang, B.-S. Wang, Z.-B. Su, *Phys. Rev. B* **2008**, *77*, 235421.
[13] P. H. Tan, W. P. Han, W. J. Zhao, Z. H. Wu, K. Chang, H. Wang, Y. F. Wang, N. Bonini, N. Marzari, G. Savini, A. Lombardo, A. C. Ferrari, *Nat. Mater.* **2012**. DOI: 10.1038/NMAT3245.
[14] A. Gambetta, C. Manzoni, E. Menna, M. Meneghetti, G. Cerullo, G. Lanzani, S. Tretiak, A. Piryatinski, A. Saxena, R. L. Martin, A. R. Bishop, *Nat. Phys.* **2006**, *2*, 515.
[15] G. Dolling, B. N. Brockhouse, *Phys. Rev.* **1962**, *128*, 1120.
[16] Z. Luo, T. Yu, J. Shang, Y. Wang, S. Lim, L. Liu, G. G. Gurzadyan, Z. Shen, J. Lin, *Adv. Funct. Mater.* **2011**, *21*, 911.
[17] X. Li, W. Cai, J. An, S. Kim, J. Nah, D. Yang, R. Piner, A. Velamakanni, I. Jung, E. Tutuc, S. K. Banerjee, L. Colombo, R. S. Ruoff, *Science* **2009**, *324*, 1312.
[18] J. Shang, T. Yu, G. G. Gurzadyan, *Appl. Phys. B.* **2012**. DOI: 10.1007/s00340-011-4853-0.
[19] J. Shang, T. Yu, J. Lin, G. G. Gurzadyan, *ACS Nano* **2011**, *5*, 3278.
[20] J. Shang, Z. Luo, C. Cong, J. Lin, T. Yu, G. G. Gurzadyan, *Appl. Phys. Lett.* **2010**, *97*, 163103.

[21] C. Cong, T. Yu, R. Saito, G. F. Dresselhaus, M. S. Dresselhaus, *ACS Nano* **2011**, *5*, 1600.
[22] C. Cong, T. Yu, K. Sato, J. Shang, R. Saito, G. F. Dresselhaus, M. S. Dresselhaus, *ACS Nano* **2011**, *5*, 8760.
[23] M. V. Klein, *Light Scattering in Solids I*, Springer-Verlag, Berlin, **1983**, pp. 169–172.
[24] S. D. M. Brown, A. Jorio, P. Corio, M. S. Dresselhaus, G. Dresselhaus, R. Saito, K. Kneipp, *Phys. Rev. B* **2001**, *63*, 155414.
[25] C. X. Cong, T. Yu, H. M. Wang, K. H. Zheng, P. Q. Gao, X. D. Chen, Q. Zhang, *Small* **2010**, *6*, 2837.
[26] L. Huang, G. V. Hartland, L.Q. Chu, Luxmi, R.M. Feenstra, C. Lian, K. Tahy, H. Xing, *Nano Lett.* **2010**, *10*, 1308.
[27] K. Ishioka, O. V. Misochko, *Ser. Chem. Phys.* **2010**, *98*, 23.
[28] S. Koga, I. Katayama, S. Abe, H. Fukidome, M. Suemitsu, M. Kitajima, J. Takeda, *Appl. Phys. Express* **2011**, *4*, 045101.
[29] H. J. Zeiger, J. Vidal, T. K. Cheng, E. P. Ippen, G. Dresselhaus, M. S. Dresselhaus, *Phys. Rev. B* **1992**, *45*, 768.
[30] G. C. Cho, W. Kiitt, H. Kurz, *Phys. Rev. Lett.* **1990**, *65*, 764.
[31] T. Mishina, K. Nitta, Y. Masumoto, *Phys. Rev. B* **2000**, *62*, 2908.
[32] Y. Yan, K. A. Nelson, *J. Chern. Phys.* **1987**, *87*, 6240.
[33] A. V. Kuznetsov, C. J. Stanton, *Phys. Rev. Lett.* **1994**, *73*, 3243.
[34] T. E. Stevens, J. Kuhl, R. Merlin, *Phys. Rev. B* **2002**, *65*, 144304.
[35] D. M. Riffe, A. J. Sabbah, *Phys. Rev. B* **2007**, *76*, 085207.
[36] T. Garl, E. G. Gamaly, D. Boschetto, A. V. Rode, B. Luther-Davies, A. Rousse, *Phys. Rev. B* **2008**, *78*, 134302.
[37] Y. Shinohara, K. Yabana, Y. Kawashita, J.-I. Iwata, T. Otobe, G. F. Bertsch, *Phys. Rev. B* **2010**, *82*, 155110.
[38] G. A. Garrett, T. F. Albrecht, J. F. Whitaker, R. Merlin, *Phys. Rev. Lett.* **1996**, *77*, 3661.